

Influence of atmosphere on phase transitions of praseodymium oxide at high temperature using high temperature X-ray diffraction and thermogravimetry

Naoki Wakiya, Sung-Yong Chun, Atsushi Saiki, Osamu Sakurai,
Kazuo Shinozaki, Nobuyasu Mizutani*

*Department of Inorganic Materials, Faculty of Engineering, Tokyo Institute of Technology,
2-12-1, O-okayama, Meguro-ku, Tokyo 152, Japan*

Received 29 August 1997; received in revised form 13 November 1997; accepted 30 November 1997

Abstract

High temperature X-ray diffraction analysis and thermogravimetric analysis up to 1400°C and 1500°C, respectively were used to examine the resulting phases and lattice parameters of praseodymium oxide in situ in N₂ and O₂ atmosphere. In N₂ (log(pO₂/Pa)=1.5), a superlattice reflection of the C-type rare earth structure was detected between 700°C and 1000°C before the decomposition of the defect fluorite into A-type rare earth structure. On the other hand, in O₂ (log(pO₂/Pa)=5.0), such a superlattice reflection was not observed. At the phase transition from defect fluorite (PrO_x) to A-type rare earth structure (Pr₂O₃) for the powder sample on the Pt plate heater, no selective orientation occurred for the Pr₂O₃ in N₂ (above 900°C), however, a strong c-axis orientation of Pr₂O₃ perpendicular to the Pt plate was observed in O₂ (above 1400°C). Such results have not been previously reported. Thermogravimetric analysis helped to identify intermediate phases. © 1998 Elsevier Science B.V.

Keywords: Praseodymium oxide; High temperature XRD; Thermogravimetry; Superlattice; Selected orientation

1. Introduction

In the Pr–O system, a homologous series of oxides with the general formula, Pr_nO_{2n-2} (*n*=4, 5–6, 7, 8, 9, 10, 12, ∞) [1–9], has been reported. In these compounds, θ (Pr₂O₃, *n*=4) has hexagonal symmetry with the A-type rare earth structure and the others are defect fluorite derivatives. These defect fluorite derivatives are classified into α (PrO₂, *n*=∞), β (Pr₆O₁₁, *n*=12), δ (Pr₁₁O₂₀, *n*=11), ε (Pr₅O₉, *n*=10), ζ (Pr₉O₁₆,

n=9), ι (Pr₇O₁₂) and s (a nonstoichiometric compound between Pr₆O₁₀ (*n*=6) and Pr₅O₈ (*n*=5)). Yao et al. reported that both ι (Pr₇O₁₂) and σ show the C-type rare earth related structure [9]. For the Pr–O system, phase composition isotherms between 402°C and 1050°C [2] and the phase diagram on the temperature–composition plane up to 1100°C [10] have been reported. The change of the lattice parameters under several oxygen partial pressure (log(pO₂/Pa)=2.7, 3.8, 4.1 and 4.6) was measured using high-temperature X-ray diffraction studies up to 800°C and 1080°C. In this way, many investigations have been reported in the Pr–O system, however, the maximum temperature for these analysis has been limited 1100°C and the

*Corresponding author. Fax: +81 3 5734 2519; e-mail: nmizutan@ceram.titech.ac.jp

range of oxygen partial pressure was also limited between 2.7 and 4.6 in log (pO_2/Pa).

Praseodymium oxide is widely used as one of the main dopants for ZnO varistors [11]. To fabricate a ZnO varistor, ceramic disks are usually sintered at high temperature, between 1100°C and 1500°C [12,13]. For a Pr-doped ZnO varistor, the electrical properties are drastically changed by the sintering atmosphere, i.e., ceramics sintered in O_2 show high non-linearity in I–V curves, in contrast, ceramics sintered in N_2 hardly show the non-linearity in the I–V curve [14]. In Pr-doped ZnO varistors, praseodymium oxide segregates at the grain boundary of ZnO and the drastic change of electrical property by the sintering atmosphere was ascribed to the valence state of Pr. Therefore the change of the valence of Pr in N_2 and O_2 with temperature should be clarified. This is because it has been reported that the solubility of ZnO into PrO_x is negligible in air [15], therefore in this work, it was assumed that the solubility in N_2 and O_2 was also negligible.

As mentioned above, the range of reported experimental conditions is insufficient to understand the phase chemistry of Pr-doped ZnO sintered up to 1500°C in N_2 ($\log(pO_2/Pa)=1.5$) and in O_2 ($\log(pO_2/Pa)=5.0$).

In this work, phase transitions of pure praseodymium oxide was examined in N_2 and O_2 by the high-temperature X-ray diffraction up to 1400°C and thermogravimetry up to 1500°C.

2. Experimental

Pr_6O_{11} ($PrO_{1.833}$) (99.9%, High Purity Chemicals, Japan) powder was used as starting material. Thermogravimetric (TG) measurement was carried out using a laboratory-made TG apparatus (electrobalance: TG-31 KM, Shimadzu, Japan) equipped with a furnace with a double spiral SiC heating element. Sample temperature was measured with a Pt–PtRh13% thermocouple which was set upward from the bottom of the furnace and positioned close to the sample. Powder samples were loaded in a platinum crucible (1 ml in volume) and were hung by a platinum wire (0.1 mm in diameter). The gas flow rate was 22 cm/min. The temperature was raised linearly from room temperature to 1520°C (6°C/min). After keeping at 1520°C

for 2 h, the power supply to the heater was cut and the samples were cooled to the room temperature in the TG. At first, Al_2O_3 powder with the same volume of the sample was put into the platinum crucible and the mass change measured with temperature. Using this profile, the effect of buoyancy was corrected for samples. The blank runs are carried out both in N_2 and O_2 and the TG profiles of the samples were corrected using corresponding atmosphere since the buoyancy factors depend on the atmosphere.

High temperature X-ray diffraction (HTXRD) was used to examine the change of the resultant phases and lattice parameters of the phases in situ from room temperature to 1400°C under N_2 and O_2 atmosphere. For this measurement, a high-temperature attachment (HTK10, Anton PAAR, Austria) was attached to the X-ray diffractometer (X'Pert-MPD system, Philips, The Netherlands). To measure HTXRD, powders of the samples were spread like a slurry on the surface of a platinum plate heater. Sample temperature was measured with a Pt–PtRh10% thermocouple welded at the backside of the platinum plate heater. Since platinum plate heater is easy to bend, it is very difficult to adjust the sample height level precisely. Therefore the d-values of each diffraction peak have deviations to a certain extent. The platinum lines were observed through into the X-ray pattern from room temperature up to elevated temperature, however, it was impossible to use them as correction of diffraction angles since the peaks of platinum were split into several pieces due to the growth of platinum grain. Therefore, in this work, the deviations were corrected using the error correction line determined by the least square calculation using the comparison of the measured 2θ values of Pr_6O_{11} (111), Pr_6O_{11} (200) and Pr_6O_{11} (220) diffraction angle at room temperature (25°C) with reported values in ICDD card (card number, Pr_6O_{11} : 42-1121). The correlation coefficient for the error correction line is 1.0000, therefore it is believed that this method of error correction is reliable at the room temperature. In this work, to correct the deviations at the elevated temperatures, an assumption that the error correction line determined at the room temperature can be used even at the elevated temperatures. Lattice parameters were calculated by the least-square calculation program RLC-3 [16] using the corrected diffraction angles.

3. Results

3.1. HTXRD results in N_2

It is well known that the most stable praseodymium oxide at room temperature is Pr_6O_{11} ($PrO_{1.833}$). The crystal structure of Pr_6O_{11} is basically classified as a defect fluorite structure, however, several authors have reported that very weak superlattice reflections can be observed and the true crystal structure is not cubic [1–8]. It was reported that a very long time annealing, as long as 100 days, is necessary to observe the superlattice reflection clearly [8]. In this experiment at room temperature, no superlattice reflection was detected for Pr_6O_{11} ($PrO_{1.833}$) as the reference pattern (ICDD card number 42-1121) except the slight coexistence of PrO_2 was detected. Fig. 1 shows changes of the XRD intensities with temperature for Pr_6O_{11} ($PrO_{1.833}$) in N_2 ($\log(pO_2/Pa)=1.5$). In this figure, c- PrO_x denotes the cubic compound with a defect fluorite structure. The C-type rare earth structure is a derivative of the defect fluorite structure. Fig. 1 indicates that a superlattice reflection of C-type rare earth structure can be detected between 700°C and 1000°C before the drastic decomposition of defect fluorite frame followed by the formation of hexagonal Pr_2O_3 (h- Pr_2O_3) with A-type

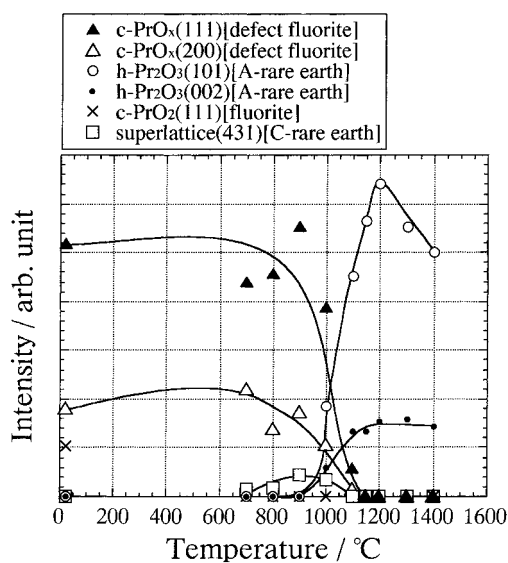


Fig. 1. Changes of XRD intensity with temperature for Pr_6O_{11} ($PrO_{1.833}$) in N_2 .

rare earth structure. Since the true lattice parameter of the C-type rare earth structure is twice as large as the original fluorite lattice, due to the ordering, the lattice parameter of the original fluorite structure was plotted in Fig. 1 for comparison. Fig. 1 also shows that cubic PrO_2 (c- PrO_2) was only detected at room temperature and was not detected above 700°C. Fig. 2 shows changes in lattice parameters with temperature for pure Pr_6O_{11} ($PrO_{1.833}$) in N_2 . For the cubic defect fluorite PrO_x (c- PrO_x), the observed change in the lattice parameter was almost linear up to 900°C and between 900°C and 1000°C a broad maximum was observed. In Fig. 2, the change of the lattice parameter of PrO_x reported by Burnham et al. [4] (at $\log(pO_2/Pa)=2.7$) was also shown. Though our measurement was carried out at $\log(pO_2/Pa)=1.5$, the change of lattice parameter with temperature for our data was in good agreement with the reported value up to 900°C, which suggests that the change of lattice parameter above 900°C is also reliable. It was also clarified that lattice parameters of both the c- and a-axes of hexagonal Pr_2O_3 (h- Pr_2O_3) with the A-type rare earth structure increases linearly with temperature. From the data, shown in Fig. 2, the linear coefficient of expansions between 1000°C and 1400°C can be calculated to be 23.7×10^{-6} and 13.6×10^{-6} for the c- and a- axes, respectively. These values are slightly larger than the reported linear coefficient of expansions, i.e., 20.7×10^{-6} for the c-axis and 9.9×10^{-6} for the a-axis measured at 900°C [4].

3.2. HTXRD results in O_2

Fig. 3 shows changes of the XRD intensities with temperature for Pr_6O_{11} ($PrO_{1.833}$) in O_2 ($\log(pO_2/Pa)=5.0$). In O_2 , PrO_x with a defect fluorite structure was continuously observed up to 1400°C. For PrO_x , the intensities of the diffraction peak drastically depended on the direction, e.g., the intensity of (200) of the PrO_x was constant up to 1350°C and it decreased at 1400°C, on the other hand, the intensity of (111) was almost constant up to 1100°C then it drastically increased with temperature up to 1350°C and suddenly dropped at 1400°C. This indicated that the (111) plane PrO_x has selective orientation. At 1400°C, PrO_x transformed into Pr_2O_3 with an A-type rare earth structure, however, only the (002) peak was strongly observed and the (101) plane, which is the

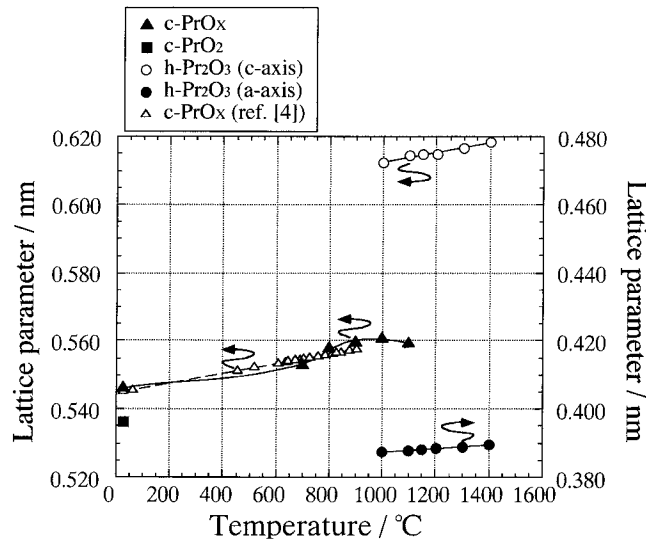


Fig. 2. Changes of lattice parameters with temperature for Pr_6O_{11} ($\text{PrO}_{1.833}$) in N_2 ($\log(p\text{O}_2/\text{Pa})=1.5$). Lattice parameters reported by Burnham et al. [4] were also shown ($\log(p\text{O}_2/\text{Pa})=2.7$).

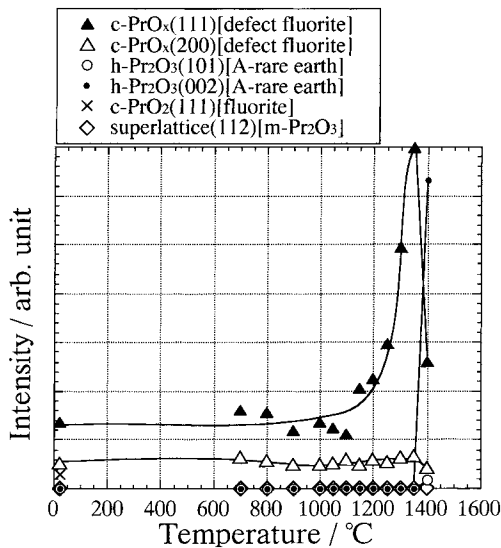


Fig. 3. Changes of XRD intensity with temperature for Pr_6O_{11} ($\text{PrO}_{1.833}$) in O_2 .

strongest intensity peak for powder X-ray diffraction, was only a trace. This indicated that PrO_X with the defect fluorite structure having a (111) orientation transformed into Pr_2O_3 with an A-type rare earth structure having the (002) orientation. It should be mentioned that formation of a superlattice reflection

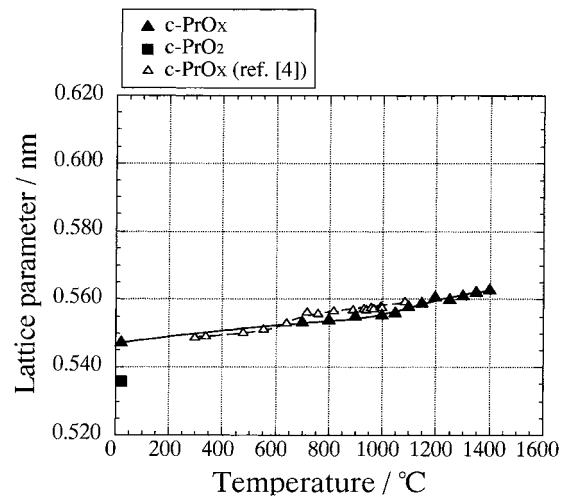


Fig. 4. Changes of lattice parameters with temperature for Pr_6O_{11} ($\text{PrO}_{1.833}$) in O_2 ($\log(p\text{O}_2/\text{Pa})=5.0$). Lattice parameters reported by Burnham et al. [4] were also shown ($\log(p\text{O}_2/\text{Pa})=4.6$).

peak of the C-type rare earth structure that was detected in N_2 was not detected in O_2 . Fig. 4 shows changes of lattice parameters with temperature for pure Pr_6O_{11} ($\text{PrO}_{1.833}$) in O_2 . This figure indicated that the lattice parameter of PrO_X with the defect fluorite structure increased linearly up to 800°C and a inflec-

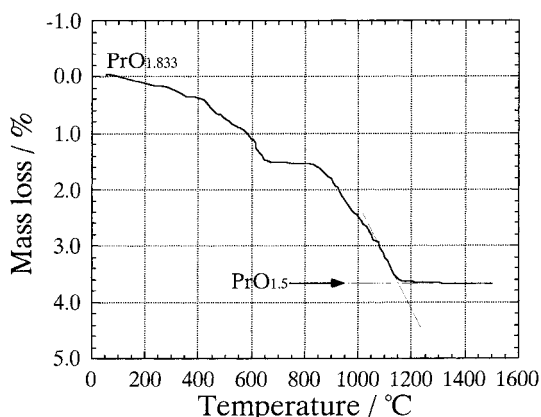
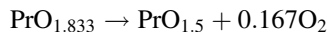


Fig. 5. Changes of mass loss with temperature for $\text{PrO}_{1.833}$ in N_2 .

tion point was observed at 900°C . In Fig. 4, the reported values of lattice parameters up to 1100°C were also shown [4]. Since our measurement was carried out in O_2 ($\log(p_{\text{O}_2}/\text{Pa})=5.0$), data obtained at the highest oxygen partial pressure ($\log(p_{\text{O}_2}/\text{Pa})=4.6$) was used for comparison. Comparing our data with the literature, the dependence of the lattice parameter on temperature agreed well except that a small inflection point was observed at 650°C in the literature but at 900°C for our data.

3.3. TG results in N_2

Fig. 5 shows the change of mass loss with temperature for $\text{PrO}_{1.833}$, in N_2 . This figure indicates that an apparent intermediate plateau can be observed between 662°C and 836°C (mass loss is 1.53%). Above 836°C , the mass decreased continuously up to 1147°C and was constant above 1147°C . This fact suggests that β (Pr_6O_{11} ($\text{PrO}_{1.833}$)) was completely reduced to q (Pr_2O_3 ($\text{PrO}_{1.5}$)) at 1147°C in N_2 . The theoretical mass loss according to the following reaction:



is 3.13%. However, as shown in Fig. 5, the value of the actual mass loss on heating of $\text{PrO}_{1.833}$ was 3.66%. The powder of $\text{PrO}_{1.833}$ used in this experiment could have adsorbed water, praseodymium hydroxide or praseodymium carbonate around $0.5 \pm 0.03\%$. In addition, as mentioned above, the coexistence of slight PrO_2 could be detected by the X-ray diffraction.

Table 1

Theoretical mass difference from $\text{PrO}_{1.833}$ for several praseodymium oxides

n in $\text{Pr}_n\text{O}_{2n-2}$	Designation	Composition	Theoretical
2	β	$\text{PrO}_{1.833}$	0.00
11	δ	$\text{PrO}_{1.818}$	0.14
10	ϵ	$\text{PrO}_{1.800}$	0.31
9	ζ	$\text{PrO}_{1.778}$	0.52
7	i	$\text{PrO}_{1.714}$	1.11
6	σ	$\text{PrO}_{1.667}$	1.63
5	σ	$\text{PrO}_{1.600}$	2.19
4	θ	$\text{PrO}_{1.500}$	3.13

Therefore the reason why the mass loss was larger than the theoretical value can be ascribed to these factors. Therefore the value of mass loss should be corrected by subtracting 0.53% because the difference between observed value (3.66%) and theoretical value (3.13%) was 0.53%. Therefore, the corrected mass loss at the plateau (between 662°C and 836°C) was calculated to be 1.00%. Table 1 shows theoretical mass difference between $\text{PrO}_{1.833}$ and several praseodymium oxides. Table 1 suggests that the composition at the plateau (between 662°C and 836°C) is i ($\text{PrO}_{1.714}$ ($n=7$)) based on mass changes.

3.4. TG results in O_2

Fig. 6 shows changes of mass loss with temperature for $\text{PrO}_{1.83}$ in O_2 . The mass loss of $\text{PrO}_{1.833}$ turned out to be constant at 1376°C and was 3.60%, therefore the

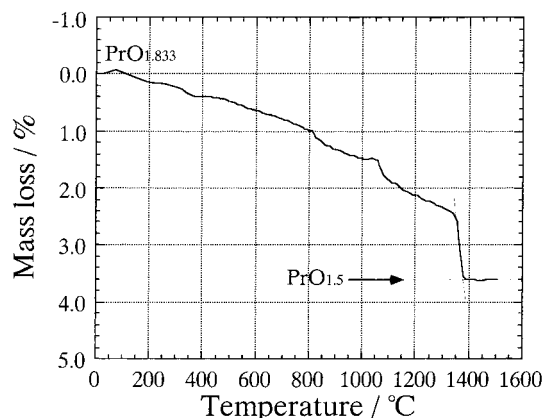


Fig. 6. Changes of mass loss with temperature for $\text{PrO}_{1.833}$ in O_2 .

profile of pure $\text{PrO}_{1.833}$ should be corrected by subtracting 0.47%. Comparing Fig. 6 with Fig. 5, it was clarified that the intermediate plateau (between 662°C and 836°C in N_2) almost disappeared and a trace of the plateau can be observed at around 1050°C. In N_2 , the mass of pure $\text{PrO}_{1.833}$ linearly decreased between 836°C (at the end of the plateau) and 1147°C. On the other hand, in O_2 , the mass of pure $\text{PrO}_{1.833}$ abruptly decreased at 1343°C, and was constant above 1376°C. The mass loss at 1343°C was 2.5%, therefore corrected mass loss was turned out to be 2.03%. Consequently, according to Table 1, the composition at 1376°C was $\text{PrO}_{1.600}$ ($n=5$).

4. Discussion

In N_2 , as shown in Fig. 1, the HTXRD results revealed that a superlattice reflection of C-type rare earth structure was detected between 700°C and 1000°C. The TG result shown in Fig. 5 indicated that this temperature range corresponded to the region between the plateau at 1.53% and on the way of mass loss at 2.5%. Applying the mass correction method mentioned Section 3.3, these values were 1.00 and 1.97%, respectively. Table 1 suggests that 1.00% corresponds to $\text{PrO}_{1.714}$ ($n=7$) and 1.97% corresponds to the nonstoichiometric region between $\text{PrO}_{1.667}$ ($n=6$) and $\text{PrO}_{1.600}$ ($n=5$). Consequently it can be mentioned that HTXRD results agreed well with TG results for the superlattice reflection peaks in N_2 .

In O_2 , as shown in Fig. 3, PrO_X shows selective (111) orientation above 1100°C. This reason is uncertain but it would be correlated to the fact that the (111) plane of cubic PrO_X with the defect fluorite structure is a close-packed plane and this plane is energetically most preferable. On the other hand, the resultant θ (Pr_2O_3 ($\text{PrO}_{1.5}$)) shows a strong (002) orientation. This phenomenon was not observed in N_2 . Since the hexagonal unit cell has anisotropy and the (001) plane is easy to grow for single crystals and thin films, since the sample in this work was powder it was more difficult to explain. One possibility to explain this phenomenon was the interaction of Pr_2O_3 with the polycrystalline Pt plate heater.

In O_2 , formation of the C-type rare earth structure observed in N_2 was not detected. This suggests that

ordering to form the C-type rare earth structure was suppressed in high oxygen partial pressures. Comparing Fig. 4 with Fig. 2, it should be mentioned that the lattice parameter of PrO_X with the defect fluorite structure linearly increases with temperature up to around 1000°C in O_2 , however the it does not linearly increase with temperature in N_2 . This difference suggests that the defect density and/or defect structure in the fluorite lattice is significantly depending upon the atmosphere.

5. Conclusions

The phase transitions of praseodymium oxide at high temperature was examined by high temperature X-ray diffraction analysis and thermogravimetric analysis in situ in N_2 and O_2 atmosphere. In N_2 ($\log(p\text{O}_2/\text{Pa})=1.5$), a superlattice reflection of C-type rare earth structure was detected between 700°C and 1000°C before the decomposition of defect fluorite into A-type rare earth structure. On the other hand, in O_2 ($\log(p\text{O}_2/\text{Pa})=5.0$), such a superlattice reflection was not observed. At the phase transition from the defect fluorite (PrO_X) to the A-type rare earth structure (Pr_2O_3) for the powder sample on the Pt plate heater, no selective orientation occurred for Pr_2O_3 in N_2 (above 900°C), however, a strong c-axis orientation of Pr_2O_3 perpendicular to the Pt plate was observed in O_2 (above 1400°C). Such a result has not been previously reported. Thermogravimetric analysis helped to identify the intermediate phases. These high temperature data could help understand the phase and nonstoichiometry of praseodymium oxide above 1100°C, especially for the valence states of Pr-doped ZnO varistors.

Acknowledgements

This work was supported by the Kawakami Memorial Foundation.

References

- [1] E.Daniel Guth, J.R. Holden, N.C. Baenziger and LeRoy Eyring, 20 (1954) 5239–42.

- [2] R.E. Ferguson, E. Daniel Guth, L. Eyring, *J. Am. Chem. Soc.* 76 (1954) 3890.
- [3] E. Alesin, R. Roy, *J. Am. Ceram. Soc.* 45 (1962) 18.
- [4] D.A. Burnham, L. Eyring, *J. Phys. Chem.* 72 (1968) 4415.
- [5] J. Kordis, L. Eyring, *J. Phys. Chem.* 72 (1968) 2044.
- [6] J. Zhang, R.B. Von Dreele, L. Eyring, *J. Solid State Chem.* 122 (1996) 53.
- [7] L.G. Liu, *Earth, Planetary Science Letters* 49 (1980) 1668.
- [8] J.O. Sawyern, B.G. Hyde, L. Eyring, *Bull Soc. Chim. France.* (1965) 1160.
- [9] S. Yao, H. Tanaka, Z. Kozuka, *J. Jpn. Inst. Metals* 55 (1991) 1216.
- [10] B.G. Hyde, D.J.M. Bevan, L. Eyring, *Phyl. Trans. Roy. Soc. London, Ser. A* 259 (1966) 583.
- [11] M. Nanba, I. Nagasawa, M. Miyagawa, T. Ishii, K. Mukae, K. Tsuda, *Fuji Gihou* 47 (1974) 1.
- [12] K. Mukae, *Am. Ceram. Soc. Bull.* 66 (1987) 1329.
- [13] M. Shida, S.Y. Chun, N. Wakiya, K. Shinozaki, N. Mizutani, *J. Ceram. Soc. Jpn.* 104 (1996) 44.
- [14] A.B. Alles, V.L. Burdick, *J. Appl. Phys.* 70 (1991) 6883.
- [15] S.Y. Chun, N. Wakiya, H. Funakubo, K. Shinozaki, N. Mizutani, *J. Am. Ceram. Soc.* 80 (1997) 995.
- [16] T. Sakurai, *Universal Program System for Crystallographic Computation*, Crystallographic Society of Japan, 1967.